7. A regional approach to model water productivity

J.G. Kroes, P. Droogers, R. Kumar, W. Immerzeel, R.S. Khatri, A. Roelevink, H.W. ter Maat and D.S. Dabas

Summary

This chapter describes a step wise regional approach towards modelling of water productivity. First step is data collection and an analysis of available data. Next step integrates the available data sets into a geographical information system and derives distributed calculation units. This requires a stratification of geographically oriented data sets, which in this study were: soil properties, village boundaries and land use. Data were downscaled to a level of 30 x 30 meter to allow comparison with remote sensing data. Parameter values were assigned to the stratified units, resulting in a set of calculation units that were analysed using the SWAP model for evapotranspiration and the WOFOST model for yields. A comparison between results from SWAP model and remote sensing images was carried out showing fair results that allowed scenario analyses. Finally the developed regional model was used to calculate spatial distributed water productivity values.

7.1 Introduction

In the previous chapters two different approaches were applied to look at water productivity in Sirsa district: field scale modelling and regional scale remote sensing. The strength of modelling is that it can be used to get a better understanding of systems and processes, while remote sensing can give a swift regional and spatial distributed overview of water productivity. However, a drawback of the modelling as presented is that it is limited to isolated fields, and a drawback of the remote sensing is that there are no predicting capacities to perform scenario analysis. In this chapter we will provide a methodology where the strength of the two approaches will be combined: a framework for crop, soil and water modelling for regional water productivity analysis.

It might be clear that the development of such an approach is based on the modelling efforts presented in the previous chapters where the calibration and validation of the SWAP-WOFOST model played a dominant role. The remote sensing, as presented in Chapter 6, provided two outputs that are used here: (i) the landcover classification and (ii) the evapotranspiration and yield estimates. The latter one will be used here as a calibration reference set, while the first one is directly input to the regional modelling framework.

In addition to the results of the modelling and the remote sensing analysis, regional analyses of water productivity require extensive additional data sets. Due to a lot of Indian field research and several (inter)national projects the availability of data for the Sirsa region is relatively favourable. Data were stored in appropriate formats which enabled regional analyses using Geographical Information Systems (GIS) and databases.

This chapter gives an overview of available regional datasets and explains the method applied to come to a regional water productivity assessment. Results are presented for the seasons *rabi* and *kharif* of 2001-02, the period during which field monitoring was carried out.

7.2 Available regional datasets

7.2.1 Soils

The soil map of Sirsa (*Ahuja et al*, 2001) was digitized into 10 soil series (Fig. 7.1). For each soil profile a vertical schematization in soil horizons was based on *Ahuja et al.,* (2001). All soil types were reduced to two-layer soil types with top and subsoils based on the proportion of sand, silt and clay. Next this information was used in so-called pedotransfer functions to obtain the soil hydraulic characteristics as described in Chapter 4.

For each soil series, measurements were available of soil salinity. Soil salinity was measured as electric conductivity in a soil-water mixture and transformed into salinity in the liquid phase using Eqs. 3.1-3.3.

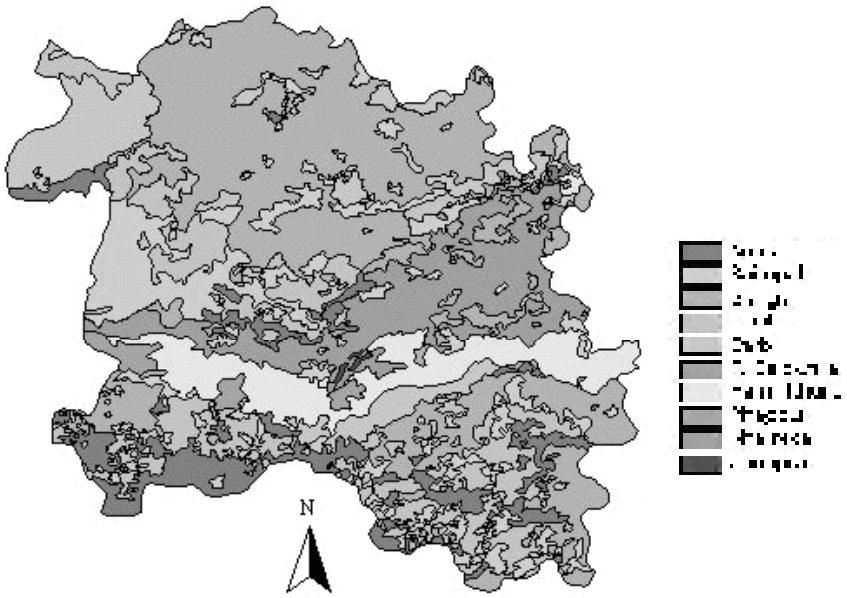

Figure 7.1 Soil map of Sirsa with 10 soil series.

7.2.2 Land use

Climatic conditions allow two crops a year, divided in two crop growing seasons; the summer growing season, called *kharif*, from May up to November and the winter growing season from November up to April, called *rabi*. The main crop during *rabi* season is wheat and during the *kharif* season rice and cotton. Other important crops are raya (oilseeds), gram (chickpea), sugarcane, fodder, guar (clusterbean) and sorghum. At present, cotton-wheat is the most dominant crop rotation in the area.

At village level information is registered with regards to agriculture management. Available data related to land use are: cultivated area, irrigated area and amount of tube wells to extract groundwater for irrigation. Because of its importance the village map was digitised.

Cropped areas were derived from remote sensing images. The combination of NOAA (high

temporal resolution) with Landsat ETM (high spatial resolution) resulted in two maps for the land use in 2002. For *rabi* season the Landsat-image of March 18, 2002, and for *kharif* season the Landsat-image of September 10, 2002, was used (Chapter 6).

7.2.3 Climate

The climate of Sirsa district is characterized by its dryness and extremes of temperature and scanty rainfall. The average annual rainfall over the period 1990-2002 is 367 mm. The region can be classified as sub-tropical, semi-arid, continental and is characterised by the occurrence of the Indian monsoon. The period from June to September constitutes the south-west monsoon. However rainfall is highly erratic both in quantity and in distribution.

.

An extensive data set with daily values measured over the period 1990 – 2002 was available from the meteorological station of Sirsa. These data include minimum and maximum temperature, relative humidity, vapour pressure in the morning and evening, sunshine hours, wind speed and rainfall (Chapter 3). The coordinates of the meteorological station of Sirsa are 29°33'39"N and 75°00'52"E.

For the period 1990-2000 rainfall measurements were available from five additional rainfall stations spread over the area, namely Ottu, Abu Shahar, Khuyan Malkanhana, Panjuana and Kalanwali. The precipitation data of the six stations were assigned to meteo-regions. For the regional analyses rainfall data were assigned to 6 meteo-regions (Fig. 7.2). For the special observation period *rabi – kharif* 2001-02, only data of Sirsa were available.

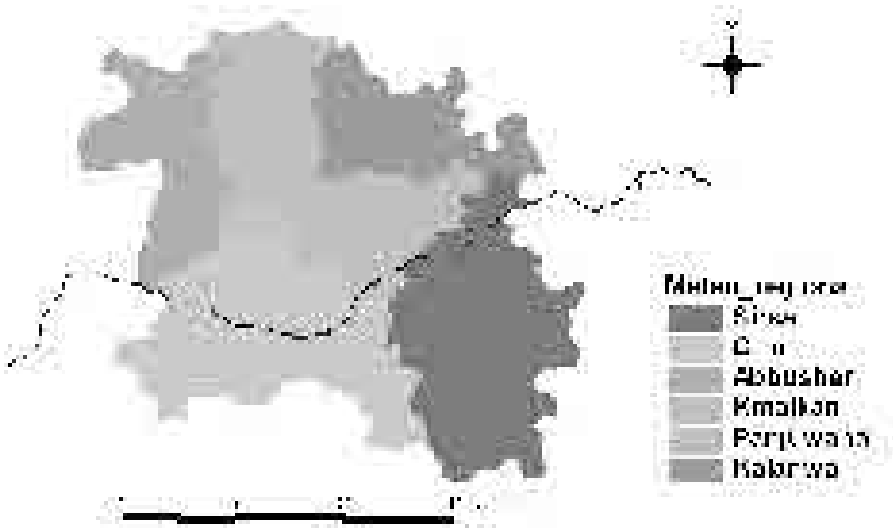

Figure 7.2 Meteo-regions based on the six rainfall stations.

7.2.4 Irrigation: groundwater

Groundwater depth

During the period 1990 – 2000 the groundwater depth was measured twice a year, in June and October, before and after the monsoon. The groundwater depth of June 2000 is given in Fig. 7.3.

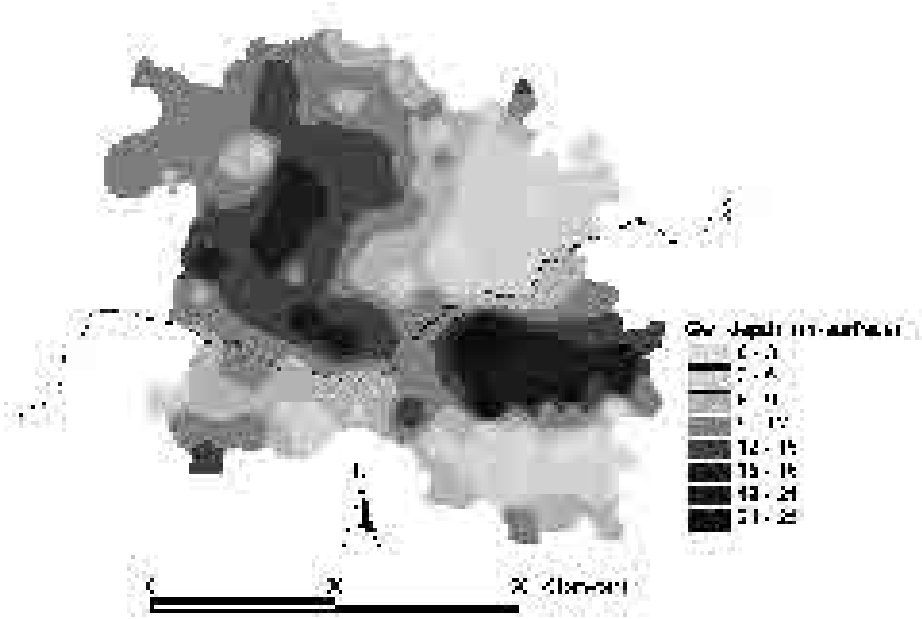

Figure 7.3 Groundwater depth of Sirsa district in June 2000 in meters below surface.

Groundwater trend

Groundwater depth fluctuates over time and space. The spatial trend of groundwater depth over the period 1990 –2000 is shown in Fig. 7.4. The groundwater trend map is based on the difference between the average groundwater depth of 1990 and 2000. The average increase of the groundwater level for entire Sirsa district amounted 9 cm y^{-1} in the period 1990-2000.

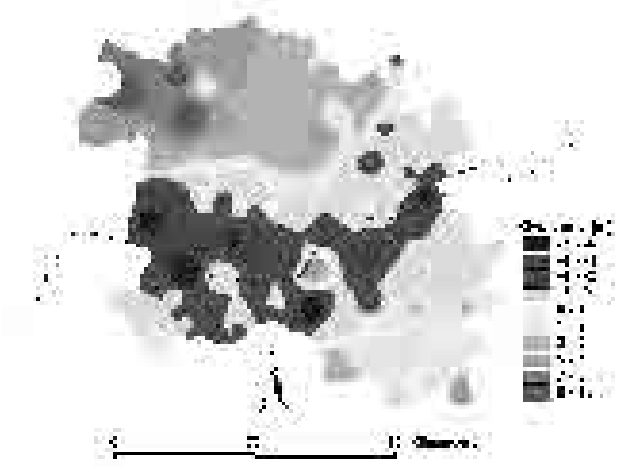

Figure 7.4 Groundwater trend (m / 10 year) of Sirsa district, calculated over the period 1990 to 2000 in meters (negative value is declining groundwater level in period 1990-2000).

Groundwater quality

For several tubewells the quality of groundwater was measured three times a year in June, October and January over the period 1982 –1995. A significant trend could not be derived from these data and therefore the groundwater quality map was based on most current values of 1995 (Fig. 7.5). Somewhat unexpectedly, the spatial distribution in this map does not correspond to the general impression that water logged areas are saline. This is partly due to the presentation form which shows interpolated values of only one year (1995) where a few extreme values may generate an unbalanced picture. A more thorough analysis of salinity levels in groundwater might be desirable but is beyond the scope of this study.

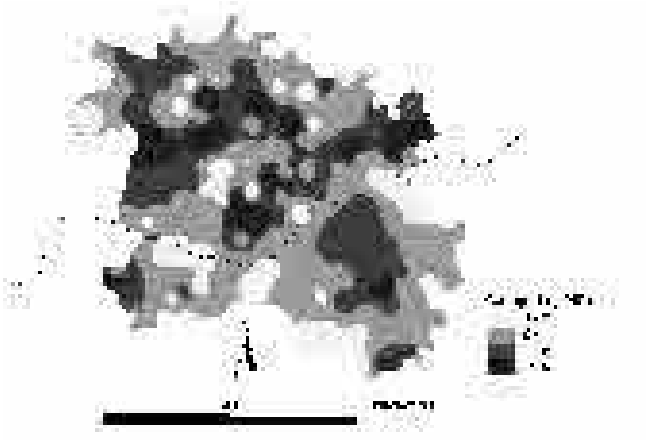

Figure 7.5 Groundwater quality of Sirsa district in dS m^{-1}, based on figures of June 1995.

The model SWAP simulates groundwater quality as a concentration of solutes, which is expressed in mg cm^{-3}. Conversion between the different units is carried out using the relation 1 dS m^{-1} = 0.653 mg cm^{-3}. Applying this relation, the values for quality of groundwater vary from 0.8 to 10.1 mg cm^{-3}. The information on groundwater depth, trend and quality maps originate from measurements of 164 observation wells spread over the Sirsa district. Interpolation between known observations was carried out to estimate values for unknown locations.

Groundwater tube wells

All farmers use tube wells and sometimes mix it with canal water to increase the irrigated area. In Sirsa district three types of tube wells can be distinguished:

- The shallow tube well, installed by local indigenous farmers. The pump capacity values vary considerably (Fig. 7.6) and were derived from Ground Water Cell (2002). Eight hours a day was assumed for working hours.
- Direct Irrigation Tubewells (DIT), installed by Haryana State Minor Irrigation and Tubewell Corporation (HSMITC). The total discharge a year for one tube well is $15 \cdot 10^6$ m^3 y^{-1}.
- Augmentation tube well, installed by HSMITC with an annual discharge of $71.5 \cdot 10^6$ m^3 y^{-1}.

For each type of tube well the number is known per village boundary. The annual discharges of the tube wells were transformed to daily discharges.

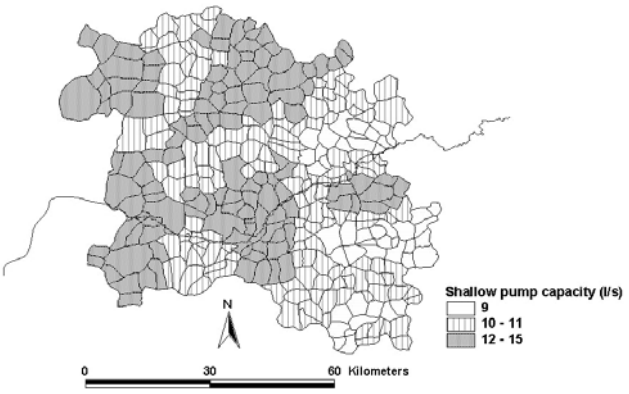

Figure 7.6 Variation in Sirsa district of pump capacity of shallow tube well in litre per second.

7.2.5 Irrigation: canal water

Sirsa district consists of four divisions (Fig. 7.7), where inflow and outflow of the main-distributaries are measured twice a day. Each division has three subdivisions. It was not possible to analyse the water availability on the more detailed level of subdivision, because most of the discharges of the minor canals were measured in gauge readings.

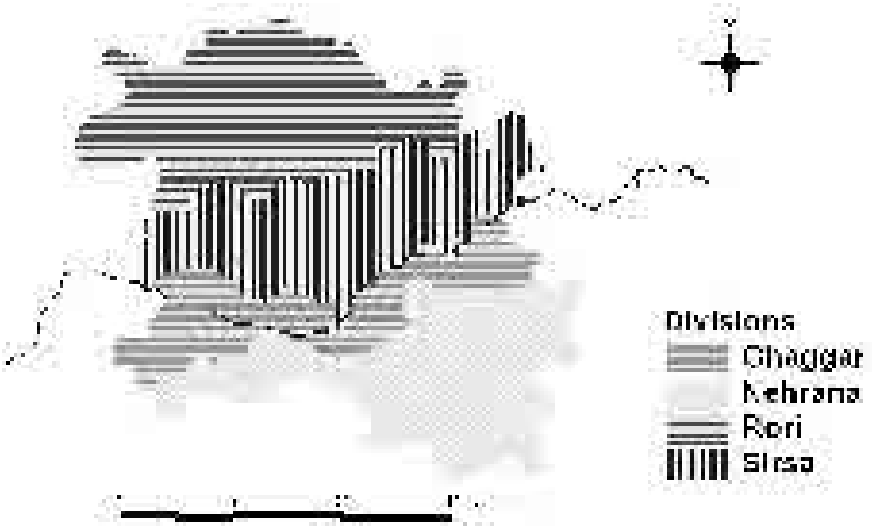

Figure 7.7 Four Water Service Divisions within Sirsa district: Rori, Sirsa, Ghaggar and Nehrana.

The quality of canal water is mostly good and constant throughout the year. In this case the quality of canal water was estimated at 0.3 dS m^{-1} or 0.2 mg cm^{-3}. Leakage losses from the main canals were estimated based on soil type according to *Roest* (1996). In his report average values of entire Sirsa district were derived by model calculations for on-farm water losses and canal seepage losses. On farm losses were in this report defined as losses caused by seepage losses from the field irrigation channels, percolation and leaching losses during field irrigation and leaching losses due to rainfall events. Based on their findings and taking into account the soil texture distribution, for each division a percentage of leakage losses was estimated (Table 7.1).

The Cultivable Command Area (*CCA*) is the area around an outlet on which the amount of canal water supply is based. The *CCA* is known per village boundary and varies throughout the years. However big differences did not occur in *CCA* during years and therefore the *CCA* values of 2001 were used for the whole calculation period.

Table 7.1 Estimation of leakage losses of main canals per water service division

Name of division	Main subsoil texture	Estimated percentage leakage losses of main canals
Rori	Loamy sand	30
Sirsa	Silt loam	20
Ghaggar	Silty Clay Loam	15
Nehrana	Sandy loam	25

7.3 Methodology

An essential part of the regional analysis was the schematization of Sirsa district into more or less homogeneous areas. These are required to allow detailed analyses of a limited amount of unique soil-water-crop systems (calculation units). To obtain these homogeneous areas a process is followed referred to as stratification. The procedure of stratification is important, because it has a large influence on amount and size of the calculation units.

The soil map and the village map were digitized and the land use map was derived from remote sensing analysis as described in Chapter 6. The land use map derived from Landsat images was considered as the basis for the soil and village maps. The pixel-size of satellite-images is 30x30 m. The soil and village maps were converted into maps with the same cell size and extent. In this way overlays of the three maps could be made without increasing the number of unique plots too much. Once the stratification procedure was finished, parameter values were assigned to the calculation units.

The SWAP-WOFOST was employed to simulate the soil-water-crop system. The regional groundwater flow has not been simulated. This was justified by the fact that the main objectives of the WATPRO study were related to crop-soil-water interactions. However, detailed groundwater modelling activities have been presented earlier (*Boonstra et al.,* 1996).

7.3.1 Stratification

Land use map

This map is a combination of land use in *rabi* season and *kharif* season. Both maps are derived from satellite-images. The *rabi*-image represents land use at 18 March 2002 and the *kharif*-image at 10 September 2002 (Chapter 6). In the original images 9 and 6 classes are distinguished, respectively for *kharif* and *rabi*-image. Reclassification was required because the local crop data were limited to the main crop rotations wheat/rice and wheat/cotton. Therefore the *kharif*-image is brought back to 3 and *rabi*-image to 2 classes (Table 7.2 and Fig. 7.8).

Table 7.2 Reclassification of land use values of remote sensing images for both *rabi* and *kharif* (old = before reclassification and new = after reclassification)

Land use *kharif* old	Land use *kharif* new	Land use *rabi* old	Land use *rabi* new
Cloud	Bare soil/rice / cotton	Bare soil	Bare soil
Cotton	Cotton	Early wheat	Wheat
Desert	Bare soil	Late Wheat	Wheat
Other crops	Rice or cotton	Oil seed	Wheat
Rice	Rice	Other crops	Wheat
Shadow/water	Bare soil/rice / cotton	Unclassified	Bare soil
Sugarcane	Rice		
Unclassified	Bare soil/rice / cotton		
Urban	Bare soil		

This implies that what is presented in this regional analyses as wheat, cotton and rice is in fact a mixture of crops (see Table 7.2) and will show deviations from reality. However, this

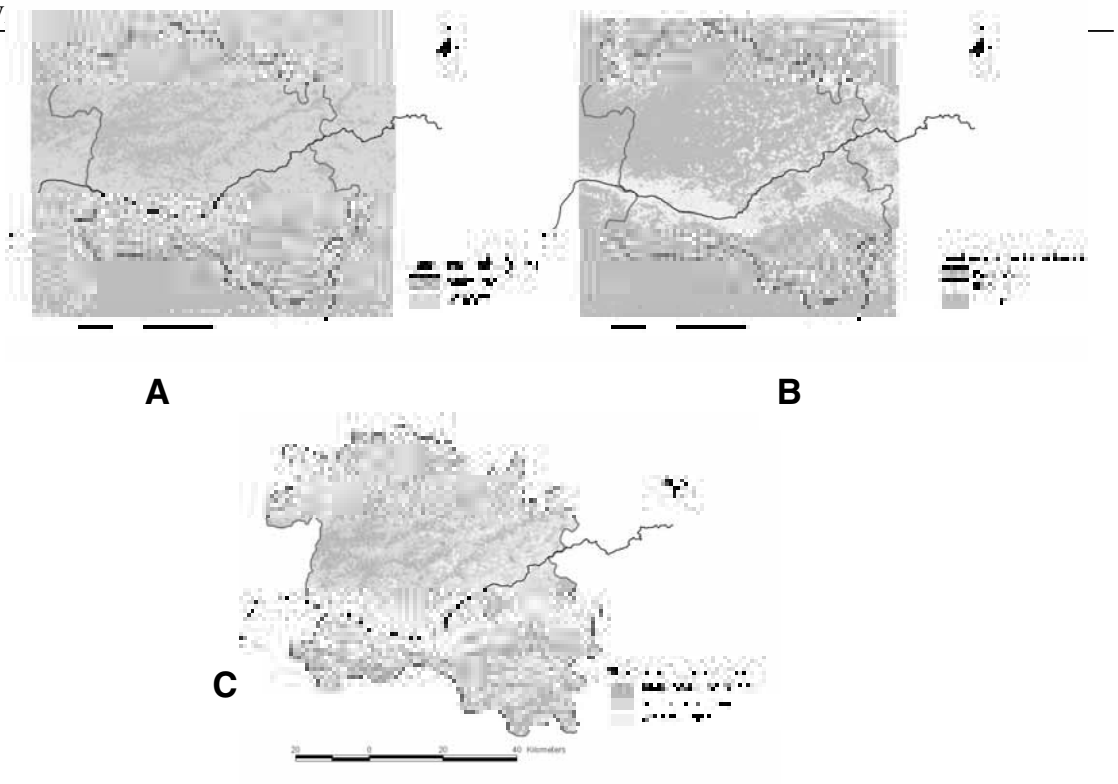

Figure 7.8 Reclassified land use for *rabi* (A) and *kharif* (B) and the resulting land use for the regional analyses (C).

simplification was assumed to be acceptable, because the remaining land uses wheat/rice and wheat/cotton are the dominating crop rotations in the area.

Soil map

The soil map, used for stratification, was derived by reclassifying the original one in which 10 soil types were distinguished, into a soil map with 6 soil types. All soil types were reduced into a two-layer soil type with a top and subsoil. Soil series with the same classification of both topsoil and subsoil, were merged (Table 7.3). The classification was based on the proportion of sand, silt and clay.

Table 7.3 Classification of soil series.

Series number	Series name	New soil type after merging	Topsoil	Subsoil
1	Nimla	1	Sand	Loamy sand
2	Saimpal	2	Sand	Sand
3	Ganga	1	Sand	Loamy sand
4	Lambi	3	Loamy sand	Sandy Loam
5	Darbi	4	Loam	Silt Loam
6	Fatehpur Baidwala	5	Silt Loam	Silt Loam
7	Harni Khurd	6	Loam	Silty Clay Loam
8	Phaggu	3	Loamy sand	Sandy Loam
9	Khaireke	5	Sandy loam	Sandy loam
10	Jhunpra	5	Loamy sand	Sandy clay loam

Village boundaries

Since many spatially allocated data were available at village level, it was decided to use a map with village boundaries as one of the maps for the stratification procedure. The total

number of villages is 323. At village level information is available, such as *CCA*, potential pump-discharge, pump-density and net-irrigated area. By using the interpolated grid maps for groundwater depth and quality, these gridded data were also available at village level.

Final stratification
An overlay of the 3 maps resulted in 2404 calculation units (Fig. 7.9). Bare soil and wheat-rice each occupy 26 % of the total area (Table 7.4) and wheat-cotton covers 48% of the area. However one should keep in mind that, due to the stratification process the different forms of land use were limited and wheat accounts for several other kinds of land use. Results presented here might therefore be different from results presented in Chapter 6.

Table 7.4 Size (in % of total area of 3878 km^2) of the land use and surface water division.

	Land use (*rabi – kharif*)			
Division	Wheat-cotton	Wheat-rice	Bare soil	Total
Ghaggar	5	10	2	16
Nehrana	12	6	9	27
Rori	17	4	8	30
Sirsa	14	7	6	27
Total	48	26	26	100

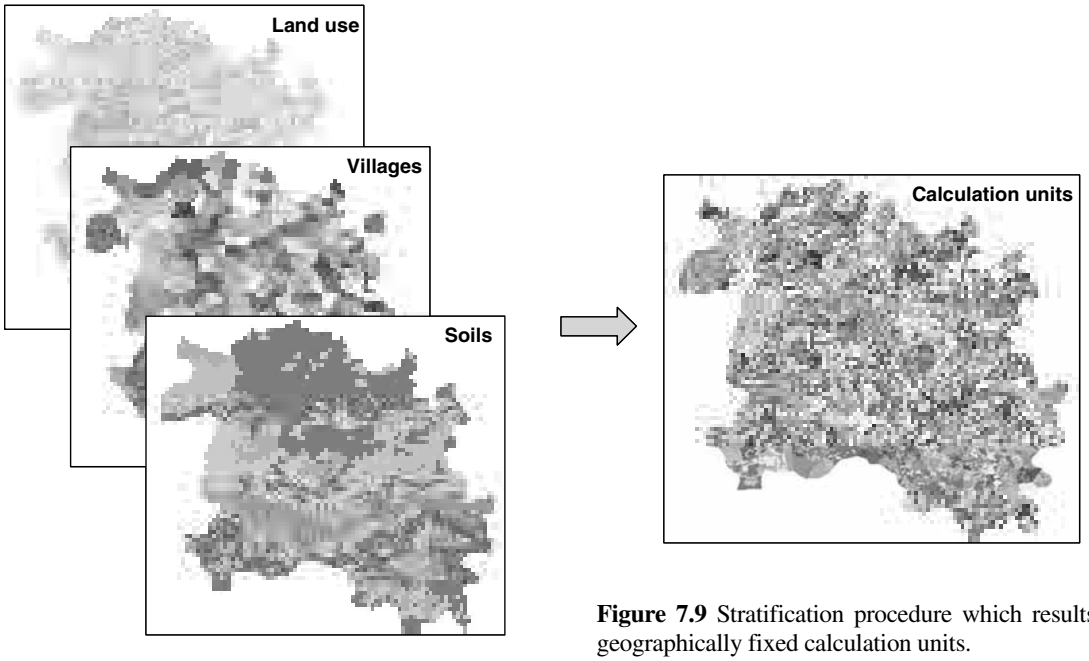

Figure 7.9 Stratification procedure which results in geographically fixed calculation units.

7.3.2 Parameterisation

Once the calculation units were fixed, parameter values had to be assigned.

Climate/Weather
Daily weather data were used. Within the Sirsa district the meteorological station of Sirsa is the only station with extensive weather data; these were applied to calculate evapotranspiration for the whole area. Precipitation data from the 6 stations were assigned to

calculation units within corresponding meteo-regions. The SWAP model requires the following weather data as input: shortwave radiation, minimum and maximum temperature, humidity expressed as vapour pressure, wind speed and precipitation.

The data obtained from the meteorological station Sirsa showed some missing values. These missing values were filled up using a statistical comparison with data from the meteorological station of Hisar. Especially sunshine hours and wind speed were adapted from Hisar. For the years 2001 and 2002, the data of the Sirsa station were applied to the whole region.

Table 7.5 Annual supply of canal water per division where *L* is leakage losses from the main canals.

Division	Water sup. (m^3 y^{-1})	*L* (-)	Water sup. (m^3 y^{-1})	*CCA*/ div. (ha)	Annual depth (mm)	Annual depth (incl. losses) (mm)
Rori	725,141,913	0.30	507,599,399	107,580	674	472
Sirsa	288,377,669	0.20	230,702,136	103,893	278	222
Ghaggar	173,031,455	0.15	147,076,736	54,589	317	269
Nehrana	297,450,662	0.25	223,087,997	118,759	250	188
Total based on divisions	1,484,001,699		1,150,101,317	384,821	386	299
Total based on in- and outflow of Sirsa district	1,208,555,398	0.225	936,630,433	384,821	314	243
According to Indo-Dutch project	2,000,000,000			555,500	360	

Irrigation - canal water

The supply of irrigation water plays an important role in water productivity. According to the *warabandi* system irrigation water is supplied homogeneously. To analyse this principle of equal water availability in the district, the divisions were taken into account. Per village the amount of *CCA* falling in one of the divisions is registered. A village might have *CCA* in different divisions. In that case the smallest part of *CCA* was assigned to the largest, so a village had only *CCA* in one particular division. With GIS it was possible to derive the map of the divisions. The borders of the divisions were fitted with the village boundaries. For each division the entry and exit points of the distributaries were determined. The difference between the discharge per day of all outgoing distributaries and the discharges per day of all entering distributaries within a division was regarded as storage per day.

Leakage losses from the main canals were estimated, as not all water stored in the area was used for irrigation water, but instead percolated to deeper soil layers (Table 7.1). In this study it was assumed that the rest of canal water was used for irrigation. To transform the discharge into irrigation depth, the total amount of *CCA* within a division was calculated. The calculation of the annual irrigation depth per division with canal water mentioned in Table 7.5 is expressed as:

$$D_{cw} = \frac{(1-L)\sum_{n=1}^{365}(Q_{inflow,\,n} - Q_{outflow,\,n})}{10\sum^{Div.} CCA_{vill}} \qquad (7.1)$$

where D_{cw} is irrigation amount of canal water per year per division (mm y^{-1}), Q_{inflow} is discharge of incoming distributaries (m^3 d^{-1}), $Q_{outflow}$ is discharge of outgoing distributaries (m^3 d^{-1}), L is fraction leakage losses of canal system (-), n is day number, and CCA_{vill} is Cultivable Command Area of a village (ha), which is summed over the division. For the *CCA* as well for the discharges of the main canals data of 2001 were used. The annual depth of canal water per division varies from 472 mm in the north to 188 mm in the south of Sirsa district. According to the Indo – Dutch project the size and water supply is larger than the values calculated with division information, because it was based on the Sirsa district, which is slightly larger than Sirsa District. Besides, the water supply in this project was based on figures of 1996, which was a wet year. The reason that the annual depth in the most northern division is still higher than the other divisions, despite the higher percentage leakage losses, is probably due to the fact that this region is compensated for the lower quality of groundwater.

A fixed irrigation schedule was used. This means that a fixed date and fixed depth is described. For each division the amount of canal water (m^3 d^{-1}) was calculated, including some leakage losses as explained above. Next these values were transformed into an irrigation depth by dividing over the area of *CCA* per division.

Groundwater
The total maximum groundwater discharge per day per block was calculated based on the density of the various tube wells (deep and shallow). Villages without data received a ground water discharge based on shallow and deep tube wells.

The final irrigation supply per calculation unit is the sum of groundwater supply from the nearest village and canal water supply from the division. For each crop-rotation irrigation days were determined based on field observations. On irrigation days water was supplied per calculation unit in the following way:

$$D_I = \frac{Q_{canal} CCA}{A_{crop}} + \frac{Q_{gw}}{10 A_{crop}} \tag{7.2}$$

where D_I is total irrigation depth (mm d^{-1}), Q_{canal} is canal water discharge (mm d^{-1}), *CCA* is Cultivable Command Area (ha), A_{crop} is cropped area derived from remote sensing images (ha) and Q_{gw} is maximum groundwater discharge (m^3 d^{-1}).

One week before and one week after the irrigation date, the calculated daily irrigation depth is assigned to that particular date. As a result of a mismatch between remote sensing data (A_{crop}) and statistical data obtained from local governments (maximum groundwater discharge derived from tube wells) an upper limit of D_I had to be defined. When a small area has a relative high maximum groundwater discharge, unrealistically high values of total irrigation depth per day could be assigned. Therefore a maximum irrigation depth of 80 mm d^{-1} has been used.

Next to the quantity of irrigation water, the quality of irrigation water was taken into account as a weighted average based on depth and quality:

$$C_I = \frac{C_{gw} D_{gw} + C_{cw} D_{cw}}{D_I} \tag{7.3}$$

where C_I is quality of irrigation water (mg cm^{-3}), C_{gw} is quality of groundwater (mg cm^{-3}), D_{gw} is depth of groundwater supply (mm), Q_{cw} is quality of canal water (mg cm^{-3}), and D_{cw} is depth of canal water supply (mm).

Crop

For the regional analysis emergences dates of crop growth and periods of irrigation scheduling were determined by means of average values obtained from the farmer fields. These dates for the crops wheat, cotton and rice are listed in Table 7.6. The number of irrigation applications was spread over the period between the first and last irrigation according to local observations.

Table 7.6 Croping patterns, based on average of farmer fields

Crop-rotation	Emergence	End	First irrigation	Last irrigation	Number of Irrigation applications
Wheat	01-11	24-04	03-11	07-04	8
Rice	20-06[(1)]	9-10	20-06	22-9	25
Cotton	01-05	31-10	10-05	19-9	4

[(1)] Transplanting

Because of the close interaction between water availability, *LAI* development and *DM* production, crop growth was simulated with WOFOST. The WOFOST module was calibrated for wheat, cotton and rice with data from local experiments. For light use efficiency and maximum CO_2-assimilation rate of wheat and cotton lower values were used than obtain during calibration in order to take into account, implicitly, the effect of management. Using WOFOST we calculated potential above ground *DM*, water limited above ground *DM*, potential *DM* production in storage organs, and water limited *DM* production in storage organs. In case of bare soil only soil evaporation was calculated.

Soil

For each soil layer defined in the soil profile, the relations between the soil water pressure head, the soil moisture content and the unsaturated hydraulic conductivity should be specified. All soil types were reduced into a two layer soil type since the actual evaporation, like surface soil moisture, is usually controlled by only the top few centimetres of soil (*Jhorar*, 2002). The topsoil exits of first 15 centimetres and the subsoil of 3.85 meter. In this study the Mualem - Van Genuchten functions were applied to describe the soil physical relations (Eqs. 4.9 and 4.10). The parameter values were taken directly from the farmer field study (Chapter 4).

Boundary conditions

A soil profile with a thickness of 4 meter was considered, assuming that most important processes occur within this upper part of the soil. For the lower boundary two conditions were distinguished: shallow and deep groundwater. Calculation units were assumed to have a shallow groundwater when the average groundwater level during the years 1999-2000 was less than 4 meter below the soil surface; all other units were assumed to have a deep groundwater level. About 10% of all units turned out to have an average groundwater less than 4 meter below surface.

For the situation with deep groundwater a free drainage condition was applied for the bottom boundary. As initial condition h = -500 cm was adopted.

For the situation with shallow groundwater the bottom flux was calculated as a function of a given hydraulic head and a vertical resistance of flow towards deeper soil layers:

$$q_{bot} = \frac{\phi_{aquif} - \phi_{gwl}}{c} \quad (7.4)$$

where q_{bot} is the flux at bottom of soil profile (cm d^{-1}), ϕ_{aquif} is the hydraulic head in a semi-confined layer (cm), ϕ_{gwl} is the groundwater level (cm) and c is the vertical resistance (d), taken here as 1000 d. The fluctuation of ϕ_{aquif} in time was assumed to have a sinusoidal wave. The amplitude of the ϕ_{aquif} sinus wave was derived from the difference between measured groundwater levels in June and October. The top of the sinus was either June or October, depending on the occurrence of the highest measured groundwater levels. Measured groundwater levels were used as initial conditions.

7.3.3 Regional modeling

For each of the 2404 calculation units, water and salt balances and crop growth were simulated. In this study the *rabi* and *kharif* seasons of the period of 2001-02 were analysed, because during this period measurements were available from both remote sensing and monitored farmer fields. The analysis was carried out using the SWAP model version 2.07 (*van Dam et al.*, 1997). A description of the SWAP and WOFOST models is presented in Chapters 4 and 5.

The SWAP model was adjusted for the simulation of paddy rice fields. An option was introduced to adjust the saturated conductivity of the soil horizon which represents the puddle layer. This layer received a value for the saturated conductivity of 1.0 cm d^{-1}. In spite of this adjustment it turned during the calibration phase that it was impossible to achieve reliable model results for the wheat-rice combination. Especially rice turned out to be very sensitive to the saturation percentage of the soil. Realistic values for rice could only be achieved after introducing a correction factor, which accounts for the uncertainty in the irrigation from groundwater tube wells. In order not to disturb the regional water balance, a sensitivity analysis was carried out for the second calculation unit. The analysis showed that a multiplication factor of 3 for the amount of tube well irrigation water would give reasonable yields without strongly influencing the leakage to deeper soil layers (Fig. 7.10). In other words, the estimation of the groundwater extraction rates was a factor 3 too low. In Chapter 9 this is elaborated and explained in more detail and the factor 3 appeared to be justified.

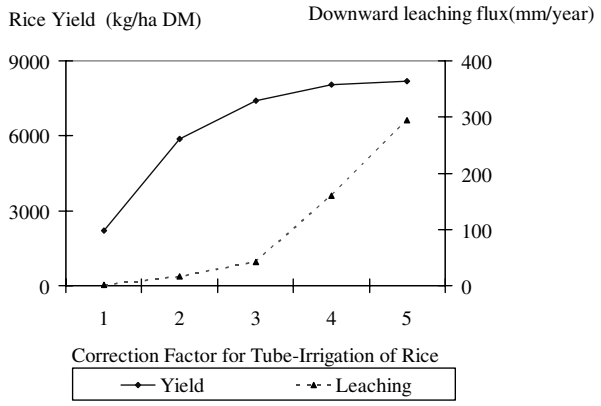

Figure 7.10 Yield and leaching as a function of a correction factor for tube irrigation of rice.

7.4 Results

7.4.1 Reference situation

The resulting water balance for the simulated period November 1, 2001 till November 1, 2002 showed that the high evapotranspiration is achieved with a large contribution of irrigation water. Rainfall and irrigation with canal water each supply about 20 % of the water. Irrigation with groundwater dominates the supply with a contribution of 60 % of the total supply to the upper part of the soil system (Table 7.7). Transpiration by the crops and soil evaporation take care of respectively 42 and 26 % of the total water discharge. Leaching (including drainage) is about 17% of the discharge.

Table 7.7 Overall water balance (mm y^{-1}), 1 Nov 2001 – 1 Nov 2002, based on the regional SWAP modelling.

IN		OUT	
Rainfall	188	runoff	5
Irrigation -–canals	210	Interception	5
Irrigation -groundwater	607	transpiration	421
		soil evaporation	260
		leaching	170
		storage	144
Total	1005	total	1005

A large part of the area (about 26%) consists of bare soil and receives no irrigation. The cropped area receives, however, high amounts of irrigated water, especially from groundwater (Table 7.8). Especially, wheat-rice receives large amounts of irrigation water through tube wells; ranging from 810 to 1465 mm/year. In the Rori division the supply from groundwater is relatively low, whereas the largest groundwater extractions occur in the Ghaggar division.

Table 7.8 Irrigation with groundwater and surface water, 1 Nov 2001 – 1 Nov 2002.

	Average depth of irrigation with canal water (mm y^{-1})		Average depth of irrigation with groundwater (mm y^{-1})	
Division	wheat-cotton	wheat-rice	wheat-cotton	wheat-rice
Ghaggar	339	245	720	1465
Nehrana	251	252	667	1285
Rori	591	531	375	810
Sirsa	247	227	684	1355
Average	334	294	624	1254

Actual evapotranspiration is highest for rice during *kharif* in the Ghaggar Division due to the large amounts of supplied of irrigation water. Lower values were calculated for the *rabi* season. Bare soils have an average evaporation of about 20 mm during *rabi* and 104 mm during *kharif*.

Transpiration reduction due to water and salinity stress is high for cotton, where an average value for T_a/T_p of 0.6 was calculated for all surface water divisions (Table 7.10). Rice hardly experiences stress in the Ghaggar division where T_a/T_p is 0.9; in the Sirsa division the

reduction for rice was most severe with the lowest value of 0.7. Wheat, growing during *rabi*, was hardly afffected by water and/or salinity stress.

Table 7.9 Actual evapotranspiration (mm) during *rabi* and *kharif*

Division	*rabi*		*kharif*		
	wheat	bare soil	cotton	rice	bare soil
Rori	238	15	653	699	99
Sirsa	240	21	663	702	105
Ghaggar	251	28	706	802	109
Nehrana	237	16	652	731	103
Average	241	20	665	731	104

Table 7. 10 Transpiration reduction (T_{act}/T_{pot}) during *rabi* and *kharif*

Division	*rabi*	*kharif*	
	wheat	cotton	rice
Rori	1.0	0.6	0.8
Sirsa	1.0	0.6	0.7
Ghaggar	1.0	0.6	0.9
Nehrana	1.0	0.6	0.8
Average	1.0	0.6	0.8

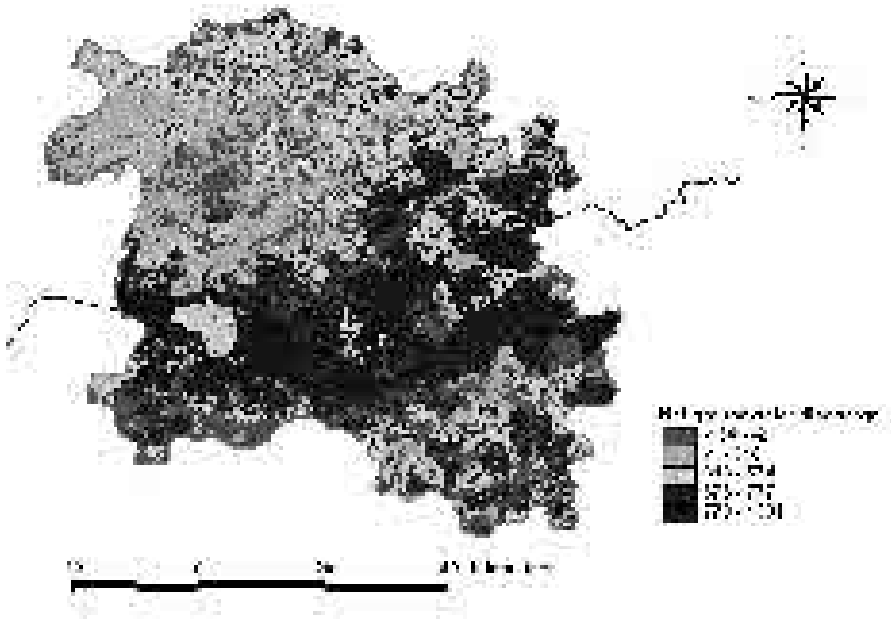

Fig. 7.11 Net groundwater discharge (mm year^{-1}) in Sirsa during 2001/02.

The net groundwater discharge was determined as the difference between the irrigation from groundwater and the downward losses to deeper soil layer. The spatial distribution of this net groundwater discharge (Fig. 7.11) shows high discharges in the areas around the Ghaggar river and low discharges in the Northern and Southern regions. Near the Ghaggar river supply of irrigation water from canal and groundwater is sufficient and the relatively shallow groundwater levels enable an easy withdrawal, which is only partly compensated by an increase in leakage.

During *rabi*, the actual yield of wheat is not reduced by any stress conditions and reaches high values of around 7000 kg ha^{-1} grain *DM* (Table 7.11). During *kharif* the yield of cotton is almost 5000 kg ha^{-1} *DM*, which is relatively high considering the water stress conditions that were faced. Simulated wheat and cotton yields were higher than the measured yields. The yield of rice is on average 5500 kg ha^{-1} *DM*, which is relatively low. This could not be improved without largely influencing the regional water balance (section 7.3.3) but was regarded as acceptable for a comparative analysis in the scenario study (Chapter 9).

Table 7. 11 Actual yield (kg *DM* ha^{-1}) during *rabi* and *kharif*.

Division	*rabi*	*kharif*	
	wheat	cotton	rice
Rori	6744	4932	5179
Sirsa	6627	4659	3931
Ghaggar	6956	4965	6816
Nehrana	6532	4751	6000
Average	6682	4799	5406

Once evapotranspiration and yield were determined, water productivity was calculated for the 3 crops. Lowest water productivity was achieved for rice in the Sirsa surface water division (Table 7.12). Highest water productivity was achieved for wheat in nearly all divisions.

Table 7. 12 WP_{ET} (kg m^{-3}) during *rabi* and *kharif*.

Division	*rabi*	*kharif*	
	wheat	cotton	rice
Rori	2.80	0.8	0.7
Sirsa	2.75	0.7	0.5
Ghaggar	2.75	0.7	0.8
Nehrana	2.75	0.7	0.8
Average	2.80	0.7	0.7

7.4.2 Comparison with remote sensing

A comparison between remote sensing results (Chapter 6) and results from the SWAP model can be analysed at various spatial scales:

- 30 x 30 m pixel, the scale of the Landsat images to which all Swap simulations were downscaled;
- villages; many input data of the SWAP model were assigned to this level;
- the entire Sirsa district.

At pixel-level (30 x 30 m) a comparison was carried out for actual evapotranspiration (ET_{act}) during the two seasons. Results on ET_{act} show a relatively good agreement for the *kharif* season (Fig. 7.12).

However the spatial accuracy of the input parameters was such that an analysis at a scale smaller than village level does not seem appropriate. Average values for *rabi* are in poor agreement (Table 7.13: 167 mm by SWAP model versus 314 mm by remote sensing), but for *kharif* the average deviation is negligible (Table 7.13: 499 mm by SWAP model versus 499 mm by remote sensing). Results were aggregated to village level and presented in Fig. 7.13

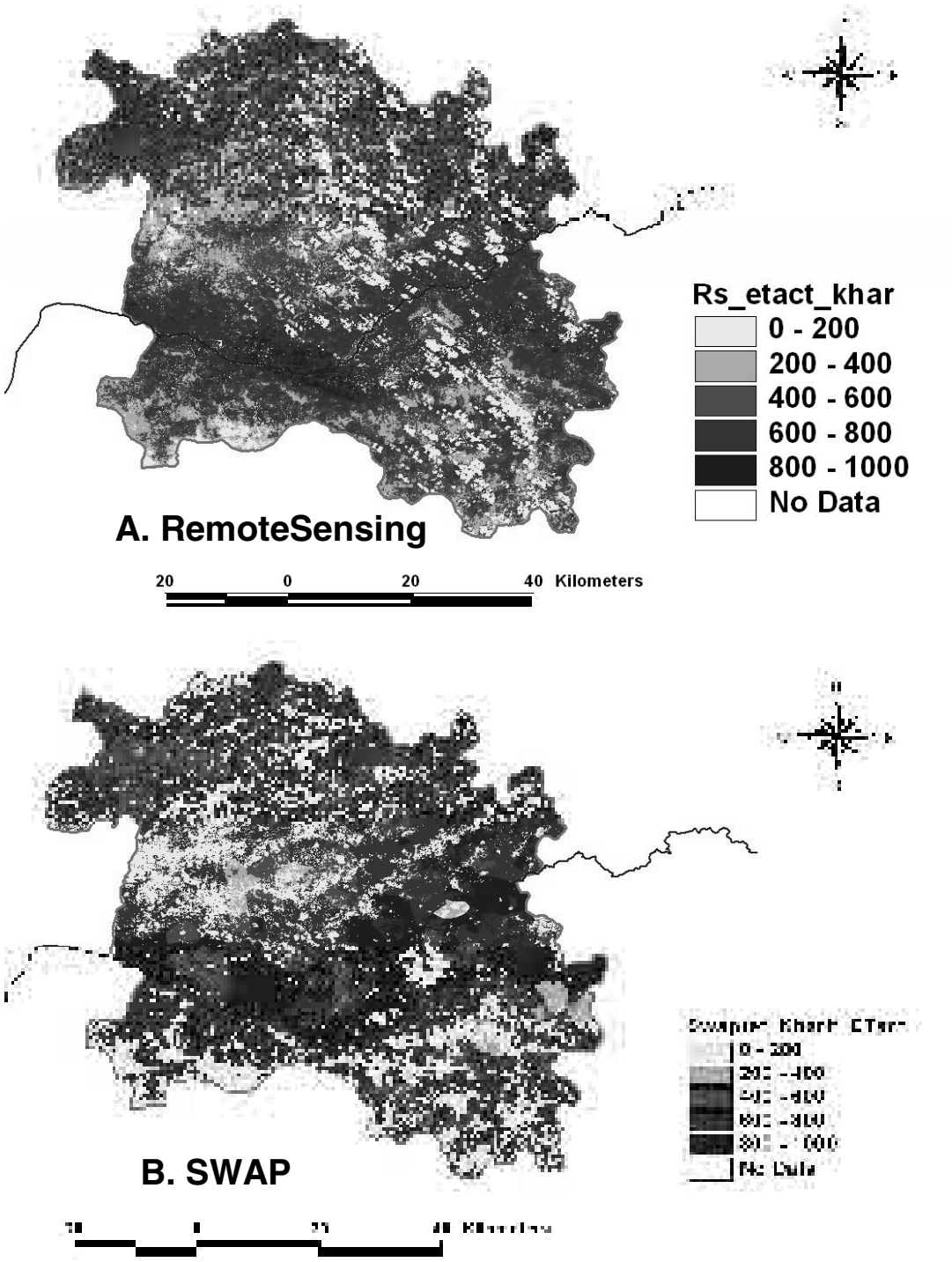

Fig. 7.12 Actual evapotranspiration (mm year^{-1}) in Sirsa during *kharif* 2002; spatial maps derived from remote sensing images (A) and the SWAP model (B).

for a comparison of actual evapotranspiration (ET_{act} in mm y^{-1}) in Sirsa during the *kharif* of 2002.

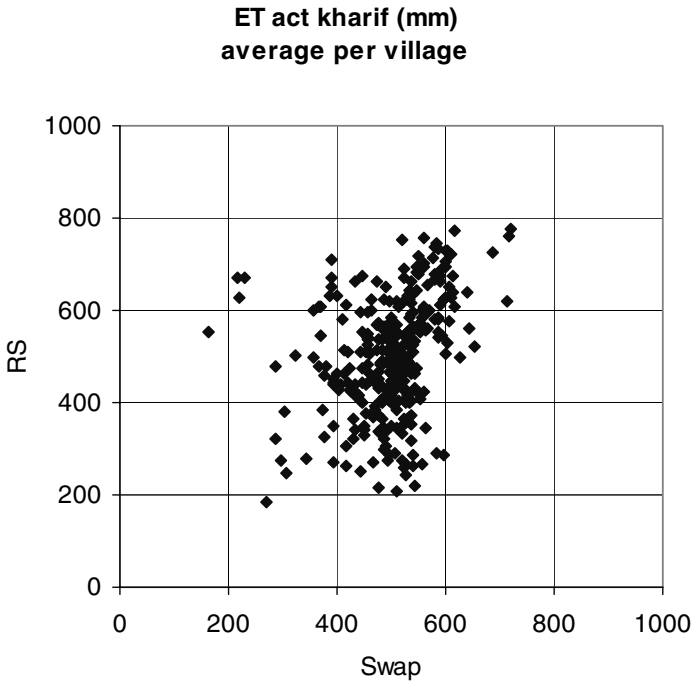

Fig. 7.13 Comparison of actual evapotranspiration (ET_{act} in mm $year^{-1}$) in Sirsa during *kharif* 2002; average values per village from remote sensing images (RS) as a function of the values from the SWAP model (Swap).

Table 7.13 Statistics on ET_a (mm y^{-1}) in Sirsa during *rabi* and *kharif* of 2001-02.

Season	Criteria	Remote sensing	Model (SWAP)
rabi	Mean value	314	167
	Standard Error	2	1
	Median	322	165
	Standard Deviation	39	20
kharif	Mean value	499	499
	Standard Error	7	4
	Median	504	509
	Standard Deviation	125	77

In spite of the differences between the results from remote sensing and SWAP model the achieved values were regarded as acceptable for scenario analyses. A more detailed analysis is recommended for future studies, which should pay more attention to dynamic interactions between the soil-water-system, regional groundwater flow and the surface water system.

7.5 Conclusions and recommendations

The following conclusions can be drawn from the regional analysis:

- The substantial amount of monitoring and data collection in India made it possible to perform the regional analysis within a relative short period of time.
- Evapotranspiration from remote sensing and the SWAP model are in good agreement during *kharif* season.

- The deviation between actual evapotranspiration from remote sensing and the SWAP model is large in the *rabi* season; this is probably due to poor irrigation water parameterization.

The following recommendations can be made:

- The database that will be distributed with this report should be maintained and extended to facilitate future regional studies.
- The spatial interaction between the various calculation units in this study was neglected; this should be improved and in future the irrigation system should become part of the stratification procedure.
- Regional groundwater was considered to be a boundary condition; a sensitivity analysis or a more detailed study should confirm the reality of this assumption.
- Modelling of puddled layers in paddy rice in rotation with wheat cultivation should get more attention; modelling of a dynamic change of hydraulic conductivity should be considered.
- The results of the regional analyses are such that it is recommended to use the modelling framework for comparative qualitative scenario studies; improvement of both instrument and data sets may enable a more quantitative approach.